2013 SNMMI Highlights Lecture: General Clinical Nuclear Medicine: Clinical SPECT/CT—Time for a New Standard of Care

From the Newsline Editor: The Highlights Lecture, presented at the closing session of each SNMMI Annual Meeting, was originated and presented for more than 33 years by Henry N. Wagner, Jr., MD. Beginning in 2010, the duties of summarizing selected significant presentations at the meeting were divided annually among 4 distinguished nuclear and molecular medicine subject matter experts. The 2013 Highlights Lectures were delivered on June 12 at the SNMMI Annual Meeting in Vancouver, British Columbia. The third presentation is included here (the first appeared in the September Newsline, the second appears on page 1N in this issue, and the last will appear in the November issue). Alan H. Maurer, MD, spoke on general nuclear medicine highlights. Note that in the following presentation summary, numerals in brackets represent abstract numbers as published in The Journal of Nuclear Medicine *(2013;55 [suppl 2]).*

It is important not only to look at the future of our specialty but to look at its evolution. I want to take a moment to assess the evolution of recent imaging technology. In general we think of the evolutionary process as quite slow. However, the evolution from the origins of clinical PET to PET/CT could be characterized as a short, 20-year revolution. In the 1980s and 1990s we had early standalone PET devices that produced images of somewhat limited quality. By 2000 the concept of hybrid PET/CT was on its way to becoming the standard of care for PET. The evolution from planar (2D) imaging to SPECT (3D) to hybrid SPECT/CT imaging has had a somewhat longer and more complex timeline. David E. Kuhl, MD, in pioneering work in the early 1970s, proposed going beyond 2D scintigraphy to cross-sectional imaging, and he was among the first proponents of SPECT. In the same time period, Godfrey Hounsfield was reporting on pioneering work on CT. The timelines of the early development of SPECT and CT are roughly synchronous. The question, then, is why has the evolutionary progress been so much slower from SPECT to SPECT/CT (>40 years) than from PET to PET/CT (<20 years)? Among possible explanations are the lack of separate reimbursement for most SPECT/CT procedures, an already large installed base of standalone SPECT units, and the need for more studies documenting clinical cost effectiveness.

One clear trend noted in the presentations at this meeting is the general acceptance of hybrid PET/CT as the standard of care. I was curious about what actually constitutes the standard of care for single-photon imaging. Many practitioners who are routinely performing PET/CT as a standard of care do not look to SPECT/CT as a similar standard. My overall conclusion, and one that I will illustrate with examples from presentations at the 2013 SNMMI Annual Meeting, is that SPECT/CT *is* a new standard of care that we should be performing on a regular basis, just as we do with PET/CT. Multiple studies at this meeting showed not only increased sensitivity, specificity, and accuracy, but increased reader confidence, decreased interobserver variability, as well as a broad range of new applications with SPECT/CT.

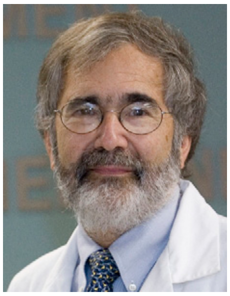

Alan H. Maurer, MD

Huellner et al. from University Hospital Zurich (Switzerland) and Lucerne Cantonal Hospital (Switzerland) reported on "Diagnostic accuracy of SPECT/CT, MRI, CT, bone scan, and plain radiographs in patients with unspecific wrist pain" [1994]. Experienced and inexperienced readers looked at images from 32 patients (Fig. 1). Experienced readers' results with SPECT/CT showed accuracy, specificity, and sensitivity of 77%, 90%, and 74%, respectively. The respective figures for MR imaging were 56%, 10%, and 65% and for planar bone scan were 44%, 70%, and 39%. Inexperienced readers' results with SPECT/CT showed accuracy, specificity, and sensitivity of 44%, 60%, and 41%, respectively. The respective figures for MR imaging were 38%, 80%, and 30% and for planar bone scan were 38%, 90%, and 28%. Plain radiographs and CT were generally poor for all readers. The researchers concluded that a more widespread use of SPECT/CT seems

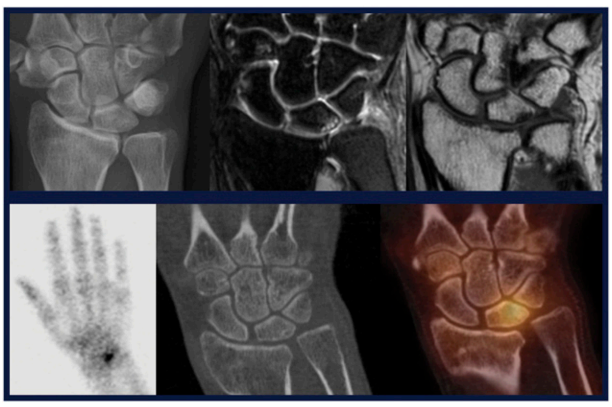

FIGURE 1. Imaging modality comparisons in patient with ulnocarpal impaction syndrome. Top row (left to right): radiograph, proton density-weighted selective partial inversion recovery MR, and T1-weighted MR. Bottom row (left to right): bone scan, CT, and SPECT/CT.

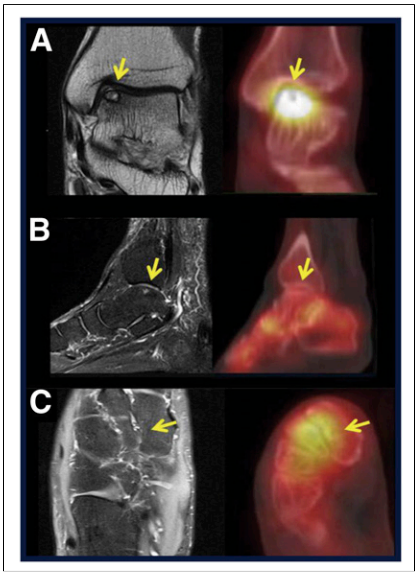

FIGURE 2. Representative comparisons of fat-saturated MR (left) and SPECT/CT (right) in ankle and foot injuries. (A) MR showed osteochondral lesion in right medial talar dome area. SPECT/CT also showed focal intense uptake in medial talar dome area, concordant with MR imaging. Resulting diagnosis was symptomatic osteochondral lesion of talus, and ankle pain was improved after arthroscopic multiple drilling of talus. (B) MR showed osteochondral lesion in right medial talar dome area. SPECT/CT showed no abnormal uptake in medial talar dome. Pain was improved after surgical removal of right calcaneal bony fragment, and talar dome lesion was nonsymptomatic. (C) MR showed no abnormality at intercuneiform joint between medial and intermediate cuneiform, although SPECT/CT showed moderate uptake.

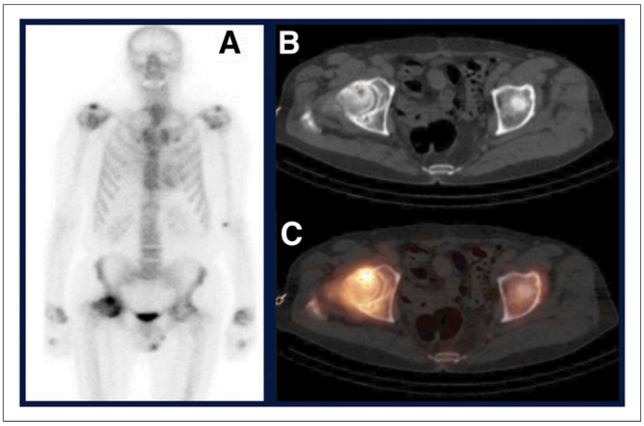

FIGURE 3. Single directed ^{11}C-methionine SPECT in 80-year-old man with prostate cancer. (A) Planar images showed increased uptake in right femur initially interpreted as malignant. (B) SPECT images. (C) Combined SPECT/CT images showed that increased uptake was caused by severe degenerative disease, confirmed at follow-up.

justified in patients with chronic disorders of the hand and wrist.

The same group of researchers also looked at "Interobserver variability in SPECT/CT, MRI, CT, bone scan, and plain radiographs in patients with unspecific wrist pain" [90]. They found that SPECT/CT imaging resulted in higher agreement between experienced readers in lesion detection and location than other modalities. They also found that agreement between experienced and inexperienced readers on lesion detection is generally poor in SPECT/CT and MR imaging, suggesting that a substantial learning curve is involved in integrating functional imaging with CT.

Ha et al. from Seoul National University Hospital (Republic of Korea) reported on "Diagnostic performance of bone SPECT/CT for traumatic injuries of ankle and foot in comparison with MRI" [422]. The study group included 47 patients with traumatic injury (137 lesions, including bone/cartilage, ligament/tendon, and joint injuries). SPECT/CT and MR were concordant in 52% of all lesions and 91% of symptomatic lesions. SPECT/CT, however, showed much higher sensitivity than MR in periarticular/joint lesions (100% and 45%, respectively). MR had slightly higher sensitivity than SPECT/CT in bone lesions (98% and 80%, respectively) and significantly higher sensitivity in ligament/tendon lesions (94% and 35%, respectively). Figure 2 shows examples from the study. Studies such as these demonstrate that SPECT/CT and MR are clearly complementary for evaluating sites of bone and soft tissue trauma.

Moving from benign to malignant bone lesion diagnosis, the study by Rasmussen et al. from the Rigshospitalet (Copenhagen, Denmark) looked at the "Value of bone scintigraphy with triple-SPECT/CT in diagnosing bone metastases" [419]. Their objective was to compare the relative value of routine (head-to-thighs) triple SPECT/CT (3-bedstop CT), SPECT alone, and mono

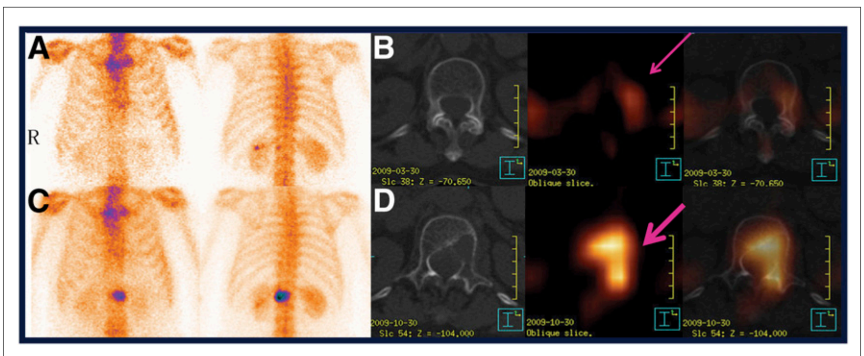

FIGURE 4. SPECT/CT in assessing solitary spinal lesion in 73-year-old woman with no discomfort 6 years after surgery for intestinal cancer and 5 years after surgery for breast cancer. (A) Initial bone scan. (B) SPECT showed lesion localized in left pedicle of vertebral arch and facet joint. SPECT/CT (right) showed area of radioactivity concentration caused by obvious degenerative changes of left vertebral facet joint, but area of radioactivity concentration in pedicle of vertebral arch was without bone damage and was diagnosed as benign. At 17-mo follow-up: (C) Bone scan. (D) SPECT and SPECT/CT (right) showed new osteolytic bone destruction of left vertebral body and pedicle of vertebral arch confirming earlier suspected involvement of the pedicle.

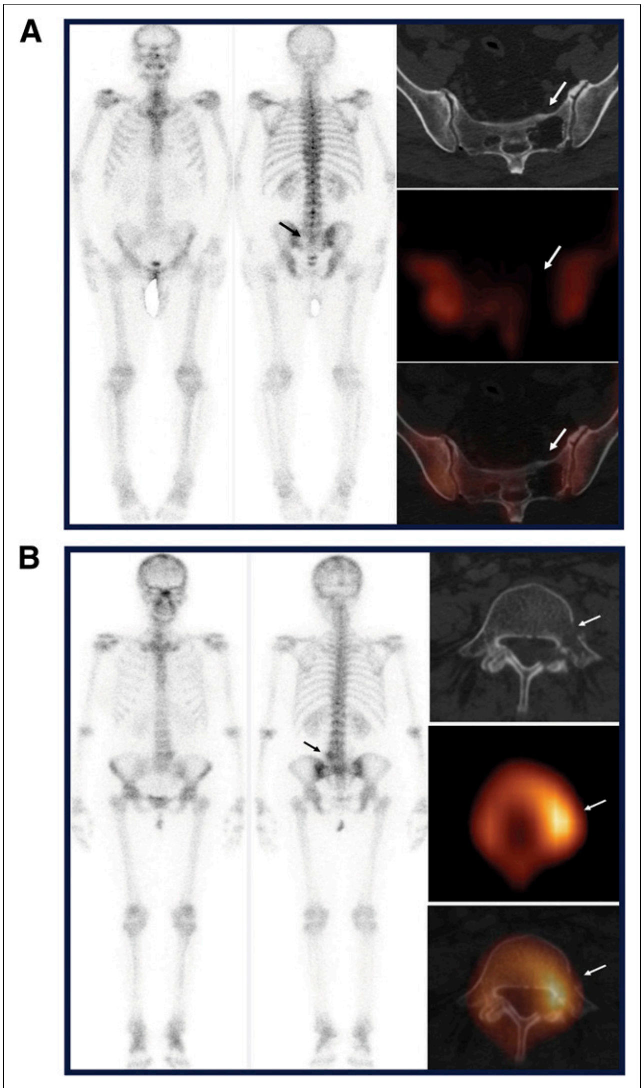

FIGURE 5. Two examples of SPECT/CT in assessing solitary spinal lesions. (A) Lesion was identified on planar imaging (left). SPECT/CT (lower right) showed clear bone cyst with sclerotic focus, moving the diagnosis from questionable malignancy to benign. (B) Planar bone scintigraphy (left) showed local abnormal radioactivity accumulation in fifth lumbar vertebra. SPECT (middle right) showed that abnormal radioactivity was in part of vertebral body and pedicle of vertebral arch. SPECT/CT (bottom right) showed wide osteolytic bone destruction at fifth lumbar vertebra. Pathology after surgery confirmed tuberculosis.

SPECT/CT (i.e., a single SPECT/CT of a localized questionable area). Their study addressed a common concern about radiation exposure with CT. The study included 68 patients with a variety of cancers (54% prostate, 38% breast, and 8% other). Although accuracy in diagnosis varied little with the different approaches, diagnostic confidence increased significantly using the single-bedstop SPECT/CT compared with the 3-bedstop SPECT/CT, reducing the number of studies interpreted as equivocal for malignancy (Fig. 3). The key point is that it is possible in questionable or equivocal areas to perform a directed SPECT/CT after a suspicious lesion has been identified on planar images, with resulting savings in both time and radiation dose.

Zhang et al. from Fudan University (Shanghai, China) reported on "Added value of SPECT/CT versus SPECT in diagnosing solitary spinal lesions in patients with extraskeletal malignancies" [1973]. Their aim was to investigate the advantages of SPECT/CT over SPECT alone in 90 patients with indeterminate solitary planar bone lesions. In results from 2 readers who scored the images, lesions on 40% of SPECT and only 6% of SPECT/CT interpretations were equivocal. SPECT/CT was also found to have significantly better diagnostic accuracy than SPECT alone (91% and 59%, respectively). Figure 4 is an interesting example from this study with follow-up.

Jiang et al. from Zhongshan Hospital (Shanghai, China) reported on the "Diagnostic value of SPECT/CT in assessing indeterminate spinal solitary lesion of patients without malignant history" [421]. The authors compared conventional planar whole-body, SPECT lesion, and SPECT/CT lesion imaging in 48 patients. They found that accuracy, specificity, and positive and negative predictive values (PPV and NPV, respectively) were much higher with SPECT/CT (79%, 50%, 76%, and 90%, respectively) than with SPECT alone (71%, 33%, 70%, and 75%, respectively) (Fig. 5). The authors concluded that SPECT/CT is an improvement over SPECT for diagnosis and evaluation of solitary lesions in the spine.

In our practice we have seen a tremendous increase in the use of labeled white blood cells (WBCs) in bone imaging, as have many institutions around the world. It has been historically difficult to differentiate osteomyelitis from Charcot neuropathic changes. Heiba et al. from the Mount Sinai School of Medicine (New York, NY) reported on "The early distinction between diabetic foot osteomyelitis and Charcot joint during initial phase leukocyte (WBC)/bone scan dual-isotope SPECT/CT imaging" [654]. The researchers looked at what additional factors seen on SPECT/CT can increase confidence about the presence of infection. The study included 22 patients with suspected osteomyelitis or Charcot joint to determine if it is possible to avoid second-day imaging with combined SPECT/CT WBC/bone marrow/colloid scan to differentiate true osteomyelitis from bone marrow hyperplasia. They compared WBC uptake patterns on first- and second-day scans, focusing on adjacent soft tissue inflammation and persistence of WBC activity (washout) (Figs. 6 and 7). It is essential to have the adequate spatial resolution from SPECT/CT to localize and identify soft tissue inflammation and marrow activity whether using single-modality WBC or dual-modality colloid imaging. The authors concluded that SPECT/CT findings in this setting may limit the need for subsequent delayed imaging in many patients and also serve to reduce radiation exposure.

SPECT/CT shows improved results even with gallium. Tamm et al. from the University of Alberta (Edmonton,

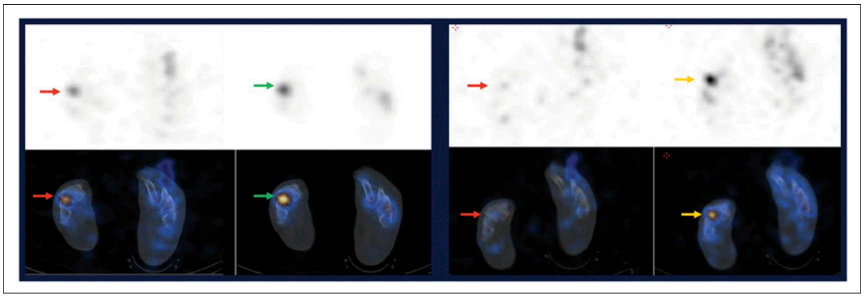

FIGURE 6. Assessment for osteomyelitis. Diabetic patient with focal uptake at right middle cuneiform bone in both WBC (red arrows) and bone (green arrows) windows of dual-isotope SPECT/CT. WBC uptake was confined to bone with no adjacent soft tissue involvement and showed washout (decreased intensity) on delayed WBC images, suggesting focal bone marrow hyperplasia and not osteomyelitis. This was confirmed by intense uptake in same location in bone marrow (yellow arrows) images.

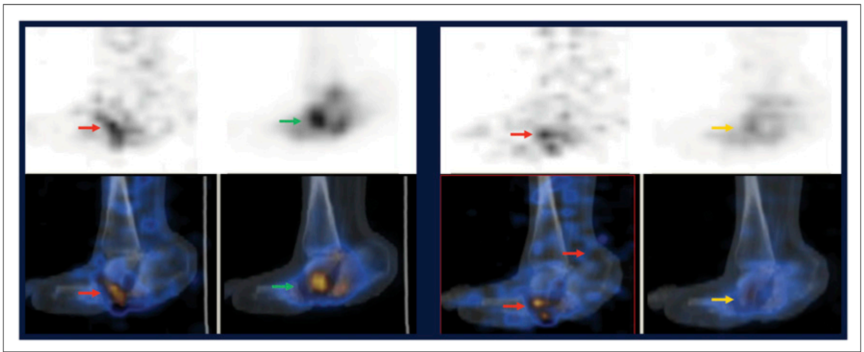

FIGURE 7. Assessment for osteomyelitis. Diabetic patient with focal uptake at left talus bone in both WBC (red arrows) and bone (green arrows) windows of dual-isotope SPECT/CT scan. WBC uptake involved adjacent soft tissue and showed no washout (no change in intensity) on delayed WBC imaging, suggesting true osteomyelitis as confirmed by lack of similar uptake in bone marrow (yellow arrows) images.

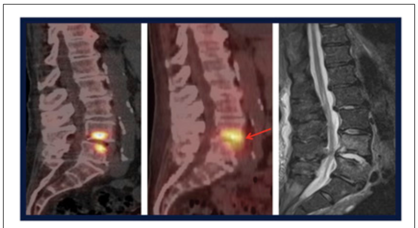

FIGURE 8. Imaging of biopsy-proven enterococcus faecalis spondylodiscitis at L4–L5. Left: increased uptake at vertebral endplates adjacent to L4–L5 disc space on bone scan SPECT/CT. Middle: discordant increased gallium uptake within disc space itself. Right: Corresponding hyperintensity in vertebral bodies and L4–L5 intervertebral disc space on T2-weighted MR imaging.

Canada) reported that "Bone/gallium SPECT-CT is equivalent to contrast-enhanced MRI in the diagnosis of infectious spondylodiscitis: a retrospective study" [653]. The retrospective study included 34 patients with suspected spondylodiscitis. Bone/gallium SPECT/CT was found to have similar sensitivity, specificity, PPV, NPV, and accuracy (94%, 100%, 100%, 94%, and 97%, respectively) to MR (94%, 100%, 100%, 80%, and 95%, respectively) (Fig. 8). Although prospective research is needed, the authors concluded that these results suggest that bone/gallium SPECT/CT is equivalent to contrast-enhanced MR imaging in the diagnosis of infectious spondylodiscitis.

Kim et al. from the Seoul National University Bundang Hospital (Seongnam-si) and the Seoul National University Hospital Boramae Medical Center (both in the Republic of Korea) reported on "The usefulness of bone SPECT/CT imaging with volume of interest analysis in early axial spondyloarthritis" [424]. The authors compared bone SPECT/CT in this setting with conventional bone scintigraphy and plain radiography (Fig. 9). The study included 15 patients with back pain being evaluated for spondyloarthritis. Sacroiliac joint-to-sacrum ratios were compared in this group with ratios from normal control participants. SPECT/CT was found to have much higher accuracy, probably because of attenuation correction and increased image contrast. The authors concluded that bone SPECT/CT is more useful than conventional bone scintigraphy in identifying sacroiliitis in axial spondyloarthritis patients, even with mild sacroiliac joint changes on plain radiography.

Other SPECT/CT Applications

SPECT/CT is beginning to prove useful in a number of new applications. Lim et al. from Emory University and the Veterans Affairs Medical Center (both in Atlanta, GA) reported on the "Feasibility of localization of gastrointestinal bleeding with ^{99m}Tc-labeled red blood cells by adding a rapid SPECT/CT to standard dynamic imaging" [586] The group assessed the value of adding the rapid SPECT/CT acquisition to traditional blood flow and dynamic images in 5 patients with gastrointestinal bleeding. SPECT was acquired with a dual-head γ camera for 10 seconds/stop over 45 or 60 stops, yielding 90–120 projections and a SPECT scan time of 9–12 minutes. CT acquisition immediately followed SPECT. Rapid SPECT/CT acquisition added diagnostic specificity for bleed location in 3 of 5 cases in which standard imaging was equivocal (Fig. 10).

An interesting report came from Takanami et al. from the Tohoku University Graduate School of Medicine (Sendai, Japan), who reported on "Visualization of the thoracic duct by 3D lymphoscintigraphy using SPECT/CT and ^{123}I-BMIPP: comparison to 3D MR lymphography" [1992]. Fatty acid is absorbed through the gastrointestinal tract and

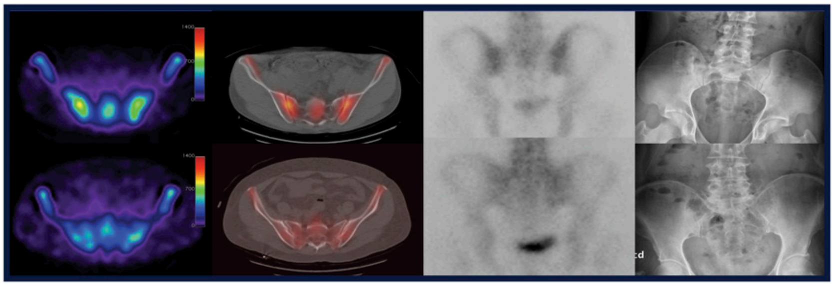

FIGURE 9. Early axial spondyloarthritis (top row) compared with images from healthy individual (bottom row). Images in patient with early spondyloarthritis include (left to right): bone SPECT and SPECT/CT showing robust periarticular uptake in sacroiliac joints, with high sacroiliac joint-to-sacrum ratio of 1.86 (right) and 1.62 (left); followed by bone scintigraphy and anterior plain radiography, which showed sacroiliac joint grade of 1 (right) and 0 (left).

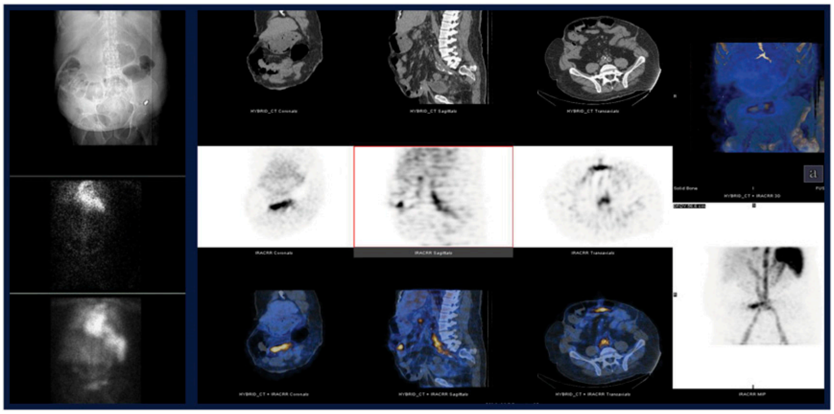

FIGURE 10. Localization of gastrointestinal bleeding with ^{99m}Tc-RBC SPECT/CT in 59-year-old man with previous history of end-stage renal disease and diabetes mellitus type 2 who presented with intermittent bloody bowel movements, hemoglobin/hematocrit of 8.9/28, requiring 2 units of packed RBCs. Left column: Static images showed diffuse uptake of tracer in midabdomen but were equivocal for bleed. Right lower images: Addition of SPECT/CT allowed better localization of gastrointestinal bleed to low riding transverse colon.

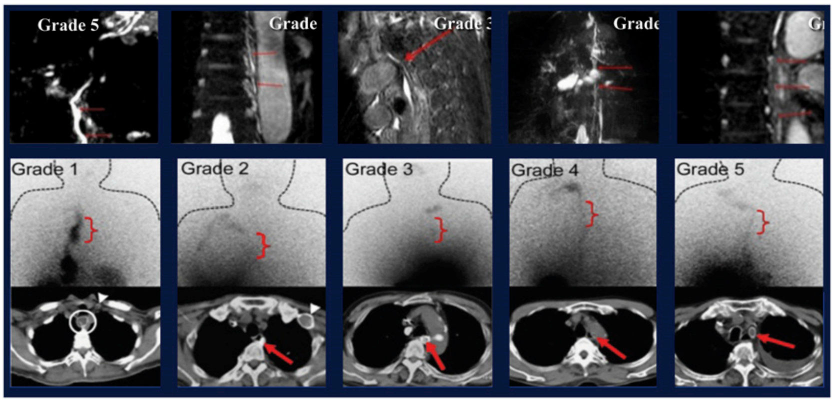

FIGURE 11. Visualization of thoracic duct by 3D lymphoscintigraphy using SPECT/CT and ^{123}I-BMIPP (bottom row, mean visualization grades 1–5) compared with 3D MR lymphography (top row, grades 5–1).

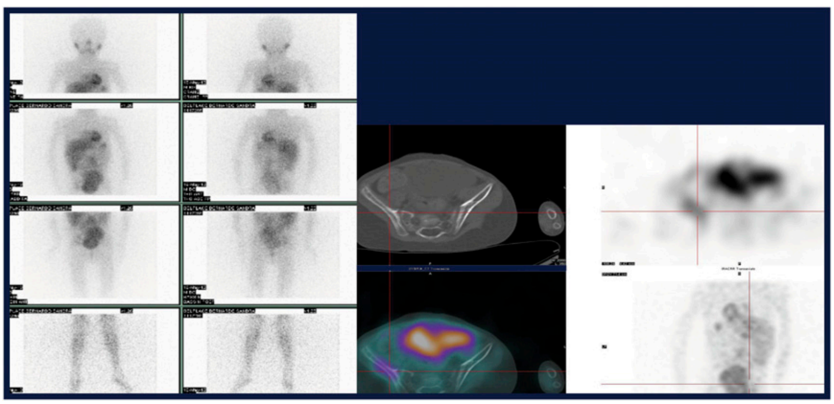

FIGURE 12. SPECT/CT in stage 4 neuroblastoma follow-up. Planar images (left) showed no bone abnormality. SPECT/CT (color image) showed right iliac bone lesion. Addition of SPECT/CT showed bony metastatic disease more precisely and allowed upstaging.

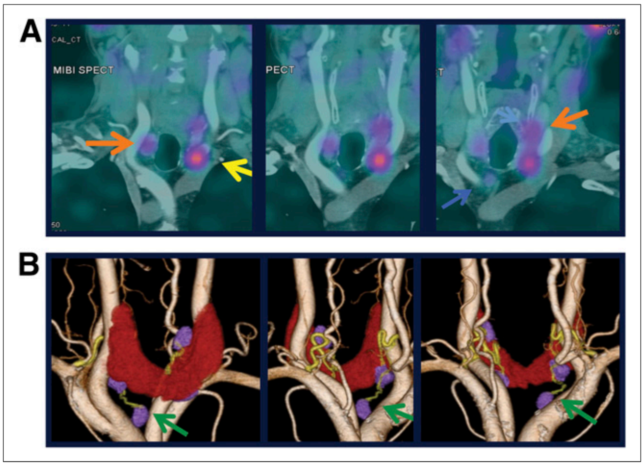

FIGURE 13. SPECT/CT and localization in hyperparathyroidism with multigland disease. (A) Sequential coronal 2D fusion images (from dorsal to ventral) of ^{99m}Tc-sestamibi SPECT and postcontrast multidetector CT showed definite uptake of sestamibi superimposed on left lower gland (yellow arrow) as well as mild uptake superimposed on left upper and right lower glands (orange arrows). However, right lower gland did not show uptake and thus was not clearly differentiated from other neck mass, such as lymph node. (B) Left anterior oblique (left) and right posterior oblique (right) projections of 3D fusion images of SPECT and postcontrast multidetector CT of parathyroid and thyroid gland in another male patient with multigland disease. Left upper gland and left lower gland can be clearly identified (purple). Right thyroid artery, arising from brachiocephalic trunk, serves as feeding artery for enlarged left lower gland. Left inferior thyroid artery reaches enlarged left upper gland.

then absorbed into the lymphatic system, ascending to the thoracic duct and producing excellent visualization and localization. This was another small study, but of 4 aberrant thoracic ducts, SPECT/CT lymphoscintigraphy demonstrated 3 (75%) and 3D MR lymphography demonstrated only 1 (Fig. 11). The authors concluded that 3D MR lymphography and SPECT/CT scintigraphy can play a complementary role in assessing the thoracic duct.

SPECT/CT in pediatric applications has also been shown to increase diagnostic accuracy and reader confidence. Wartski et al. from the Curie Hospital (Paris, France) reported that "^{123}I-MIBG SPECT/CT increases interpretation confidence in neuroblastoma" [1996]. The researchers' aim was to assess the incremental value of ^{123}I-MIBG SPECT/CT over that of planar imaging in 29 patients with neuroblastoma. In 25 of 36 examinations, planar ^{123}I-MIBG was indeterminate. Doubtful sites on planar imaging included locoregional lymph nodes, liver, pleura, distant lymph nodes, bones, and primary lesions. SPECT/CT changed the interpretation to determinate in 23 of these 25 scans (Fig. 12).

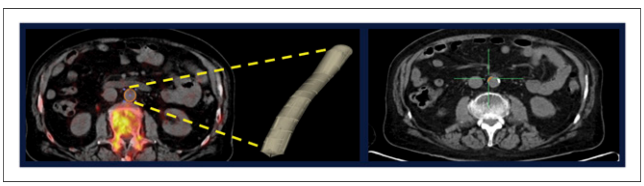

FIGURE 14. ^{18}F-NaF PET imaging in detection of early and ongoing molecular calcification and cardiovascular risk. Volumes of interest were drawn on all large arterial vessels (aorta, subclavian, carotid, iliac, and femoral arteries) to assess mean uptake (target-to-background ratio). In the same vessels, arterial calcium score was quantified.

Improved Preoperative Quantification

Knollmann et al. from the Kliniken Maria Hilf (Moenchengladbach, Germany) reported on "CT-based 3D vs. planar-derived quantification of pulmonary lobe ventilation and perfusion in preoperative lung cancer patients" [2021]. The group compared lobar ventilation/perfusion results from planar imaging with those from 3D SPECT/CT in 15 patients with poor lung function being evaluated for lung cancer resection. They found that lobar ventilation and perfusion fractions obtained by 3D quantification differed greatly from those obtained by the model-based calculation of planar scintigraphy and recommended that the 3D SPECT/CT approach should be used whenever possible.

Another new area of clinical quantification using SPECT/CT is in bone densitometry. Cachovan et al. from Friedrich Alexander Universität (Erlangen, Germany) and Siemens Healthcare (Hoffman Estates, IL) reported on "Quantitative bone SPECT with OSEM" [423]. The group used SPECT/CT to determine activity concentrations (AC) (in kilobecquerels per milliliter) of ^{99m}Tc-diphosphonate in the lumbar vertebrae in 60 women referred for bone scintigraphy. ACs were correlated with bone density in Hounsfield units and found to be in excellent agreement. Significant correlations were also found between decreasing AC and increasing age. Standardized uptake values (SUVs) were determined to be in the same range as those reported for ^{18}F-fluoride measured using PET. Additional studies are needed to demonstrate the clinical utility of this quantification approach in metastases and osteoporosis.

Secondary Fusion with Standalone Diagnostic CT 3/4D Fusion

SPECT/CT does not always have to be performed using a hybrid unit—we are often asked to perform SPECT fusion with prior CTs. Nakada et al. from the Hokko Memorial Hospital, Kamijo Thyroid Clinic, Sapporo Kosei Hospital, and Kaisei Hospital (all in Sapporo, Japan) reported that "Fusion images of MIBI SPECT and multidetector CT improve diagnostic performance of localization study in hyperparathyroidism with multigland disease" [145]. In 2010 this group was recognized with the SNMMI Image of the Year award for their work on the value of 3D SPECT/CT fusion for localizing solitary parathyroid adenomas. In the study presented this year, they compared high-resolution ultrasound, ^{99m}Tc-sestamibi scans, and multidetector CT for presurgical evaluation of multigland disease in 25 patients (8 with primary and 17 secondary hyperparathyroidism) with 78 involved glands. Fused SPECT/CT yielded

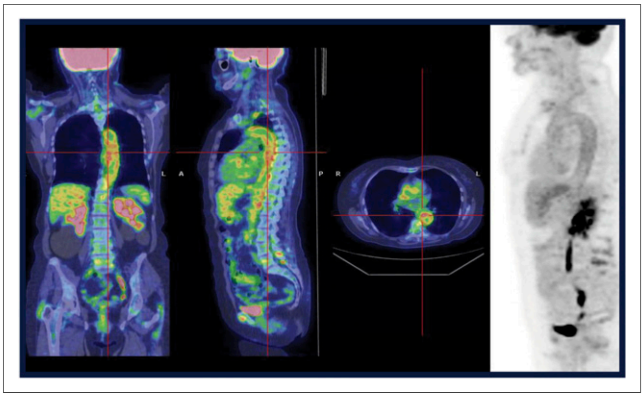

FIGURE 15. ^{18}F-FDG PET/CT in large-vessel vasculitis. PET/CT was found to correlate well with multiple clinical indices of large-vessel vasculitis disease activity.

the highest sensitivity of all modalities as well as the highest PPV (Fig. 13).

General Clinical PET

An interesting approach in vascular imaging came from Morbelli et al. from the Galliera Hospitals CNR (Genoa, Italy) and the University of Pennsylvania (Philadelphia), who reported on "Assessment of molecular calcification in the arterial wall of various cardiovascular risk subgroups by NaF-PET imaging" [182]. The group evaluated the potential role of ^{18}F-NaF PET imaging in detection of early and ongoing molecular calcification in the arterial wall in 80 patients imaged for breast or prostate cancer (Fig. 14). Cardiovascular risk (low, intermediate, or high) was determined using the Framingham questionnaire scale. Results were correlated with ^{18}F-NaF uptake and compared with results from calcium score obtained from general CT. Analyses showed that cardiovascular risk correlated with ^{18}F-NaF vascular uptake but not with arterial calcification score. Arterial ^{18}F-NaF uptake effectively distinguished the 3 cardiovascular risk groups, suggesting the feasibility of this tracer in molecular detection of early stages of arterial calcification. This is a quantifiable finding that precedes calcification as detected by CT.

Interest in FDG PET vasculitis imaging continues. Versari et al. from Santa Maria Nuova Hospital–IRCCS (Reggio Emilia, Italy) and the Istituto Ortopedico Rizzoli (Bologna, Italy) reported on "FDG PET/CT in large-vessel vasculitis: role in assessing disease activity" [184]. The group looked at 215 imaging studies in 78 patients with giant cell arteritis, Takayasu arteritis, or idiopathic aortitis. They found that PET/CT correlated well with multiple clinical indices of these diseases as well as laboratory values (Fig. 15). They concluded that ^{18}F-FDG vascular uptake is a significant and differentiating indicator of large-vessel vasculitis disease activity.

Keidar et al. from Rambam Health Care Campus (Haifa, Israel) reported on "FDG uptake in noninfected prosthetic vascular grafts: incidence, patterns, and changes over time" [650]. The group was interested in the incidence and serial patterns of ^{18}F-FDG uptake over time in noninfected grafts in relation to specific prosthetic material and location. Diffuse uptake was found in 92% of 107 noninfected vascular prostheses (7 native veins and 100 synthetic grafts) (Figs. 16, 17). The intensity of ^{18}F-FDG uptake was unchanged in synthetic grafts in sequential studies up to 16 years after surgery but decreased in native prostheses. The intensity of noninfected prostheses was higher in Dacron grafts than in other materials. The authors concluded that knowledge of the presence, patterns, and persistence of ^{18}F-FDG uptake in noninfected vascular prostheses helps to avoid misinterpretation of PET/CT studies in patients assessed for suspected graft infection.

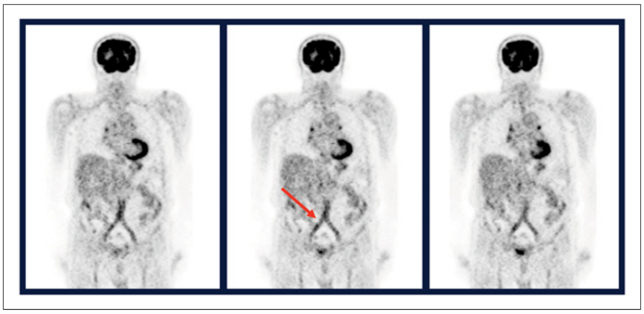

FIGURE 16. ^{18}F-FDG uptake in noninfected prosthetic vascular grafts. PET imaging of Dacron aorto-bifemoral bypass graft (arrow). Intensity of noninfected prostheses was higher in Dacron grafts than in other materials.

We have seen much interest in imaging of parathyroid adenomas using ^{11}C-choline. Orevi et al. from the Hadassah Hebrew University Medical Center (Jerusalem, Israel) reported on "Localization of parathyroid adenoma by ^{11}C-choline PET/CT: preliminary results" [144]. The group compared ^{11}C-choline PET/CT images and ^{99m}Tc-sestamibi scintigraphy before surgery in 40 patients with biochemical hyperparathyroidism. ^{11}C-choline PET/CT was found to localize parathyroid adenomas in 37 patients compared to 33 with ^{99m}Tc-sestamibi (Fig. 18).

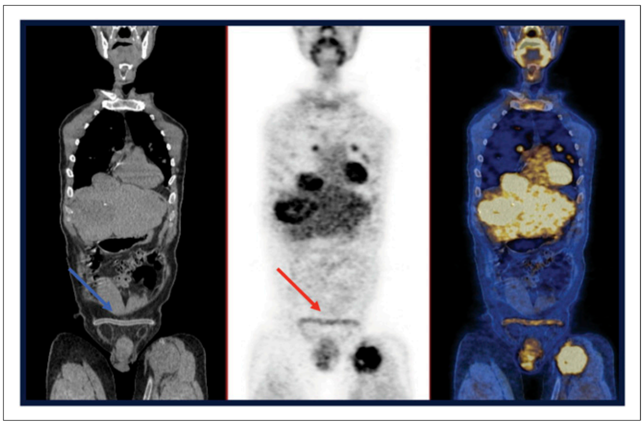

FIGURE 17. ^{18}F-FDG uptake in noninfected prosthetic vascular grafts. Goretex femoral–femoral bypass graft (arrow).

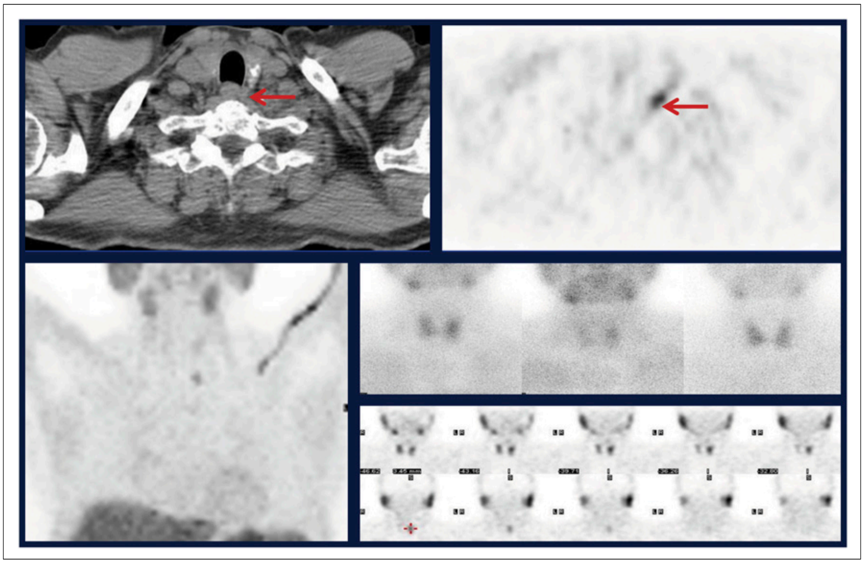

FIGURE 18. ^{11}C-choline PET/CT (top and lower left) and serial ^{99m}Tc-sestamibi scintigraphy (middle right) before surgery in patient with hyperparathyroidism. PET/CT was superior in localizing disease (arrow).

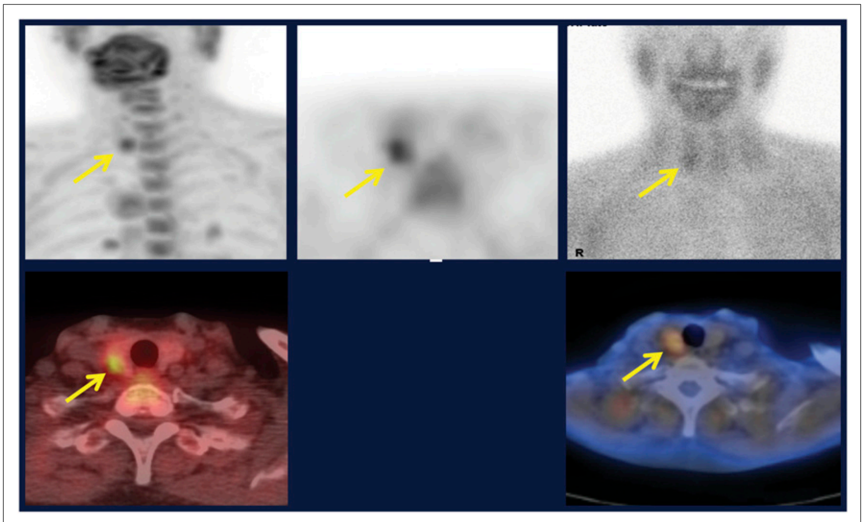

FIGURE 19. Parathyroid adenoma in 60-year-old woman. ^{11}C-methionine PET/CT (left and middle columns) and ^{99m}Tc-sestamibi SPECT/CT (right column) were found to have similar performance in localizing disease (arrows).

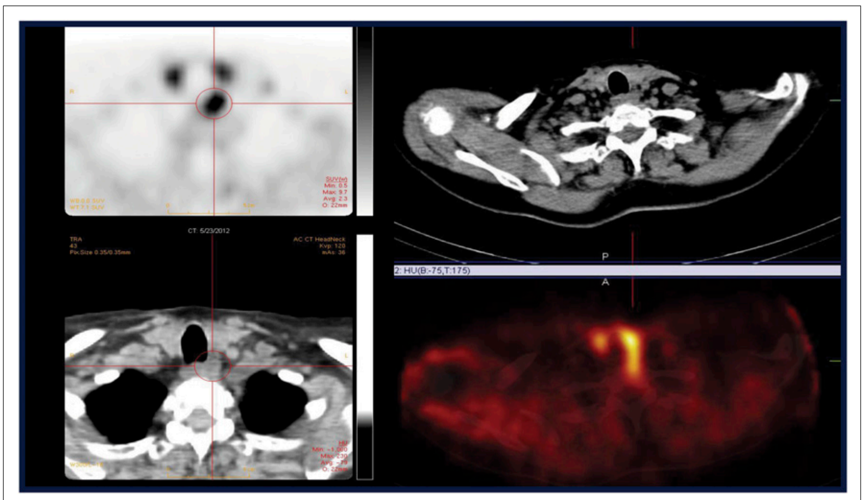

FIGURE 20. ^{18}F-fluorocholine PET/CT (left) was compared with ^{99m}Tc-sestamibi SPECT/CT (right) for preoperative localization of parathyroid adenomas. PET/CT provided clearly superior localization of adenoma at left inferior pole of thyroid gland.

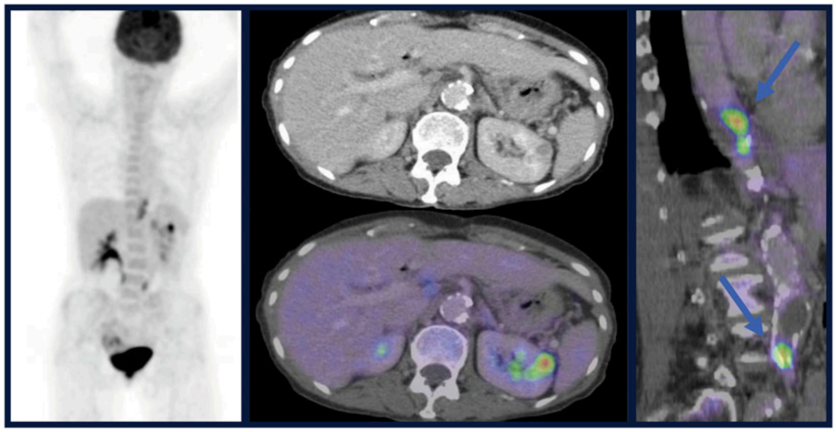

FIGURE 21. ^{18}F-FDG PET/CT in inflammation of unknown origin. Images acquired in 69-year-old woman with weight loss and recent loss of muscle strength in legs. ^{18}F-FDG PET/CT showed increased tracer uptake at edges of 2 thrombus masses in abdominal aorta and in cortex of left kidney. Postoperative pathology reported intraluminal aortal epithelioid angiosarcoma.

PET/CT also facilitated surgery in 23 of 26 patients who proceeded to surgery. Their results suggested that ^{11}C-choline PET/CT is more sensitive than ^{99m}Tc-sestamibi scintigraphy in this setting, improves confidence in image interpretation, and provides additional mapping for surgical exploration, all with significantly shorter acquisition time.

Hayakawa et al. from Kyoto University (Japan) reported on "A prospective comparison between ^{11}C-methionine PET/CT and ^{99m}Tc-sestamibi SPECT/CT for localization of hyperfunctioning parathyroid tissue" [142]. This prospective study compared the diagnostic performance of ^{99m}Tc-sestamibi SPECT and a cadmium-zinc-telluride solid-state detector with that of ^{11}C-methionine PET/CT in 23 patients (Fig. 19). No significant differences were found in sensitivity, specificity, PPV, NPV, or diagnostic accuracy with the 2 techniques.

Lezaic et al. from University Medical Center Ljubljana (Slovenia) reported on the "Usefulness of ^{18}F-fluorocholine PET/CT for preoperative localization of parathyroid adenomas" [141]. The group compared PET/CT with ^{99m}Tc-sestamibi, with a view toward facilitating minimally invasive surgery. Of 15 confirmed adenomas, PET/CT correctly localized 11 (73%) and identified the affected side in 13 (87%). SPECT localized only 5 adenomas (33%) and identified the affected side in 6 (40%) (Fig. 20). The authors concluded that although their study size was small, ^{18}F-fluorocholine PET/CT appears to be superior to ^{99m}Tc-sestamibi SPECT for localization of parathyroid adenomas, especially in cases of multiple localizations. The bottom line in all of these comparisons for parathyroid imaging is that the higher resolution of PET/CT appears to improve localization. This approach, however, has not yet entered into routine clinical use.

Outcomes and Comparative Effectiveness Research

Last year I noted that we have not done a sufficient job of supporting work with high-quality outcomes-based comparative effectiveness research. We know health care costs are rising and that the result is increased scrutiny on the effectiveness and long-term benefits of our techniques. Balink et al. from the Medical Center Leeuwarden and the University of Amsterdam (both in The Netherlands) reported on "Diagnostic utility of ^{18}F-FDG PET/CT in inflammation of unknown origin (IUO)" [651]. In this multicenter retrospective study, the group looked at the contribution of PET/CT in diagnosis of patients with IUO and also assessed C-reactive protein and erythrocyte sedimentation rate as possible predictors for ^{18}F-FDG PET/CT outcomes. The study included 140 patients with IUO, in 90% of whom ^{18}F-FDG PET/CT correctly identified or excluded a causal explanation (Fig. 21).

Edward B. Silberstein, MD, from the University of Cincinnati Medical Center (OH), and a consortium of coauthors from 15 U.S. universities reported on a "A study of the prevalence of adverse events caused by radiopharmaceuticals and adjunct interventional drugs and of trends in the utilization of radiopharmaceuticals in the United States, 2007–2011" [088]. In a carefully constructed prospective study the group looked at multiple datapoints related to adverse events in a total of 1,011,023 diagnostic studies (PET, 207,281; non-PET, 803,742) and 13,200 therapies involving radiopharmaceuticals. For the 5-year period they noted a decrease in the adverse event rates, from 3.2/100,000 dosages in 2007 to 1.6/100,000 dosages in 2011. The aggregated results were almost identical to those in a similar study led by Silberstein in 1996 *(J Nucl Med.* 1996; 37:185–192*)*, confirming the overall safety of our techniques.

Conclusion

As noted earlier, I believe that just as we have established PET/CT as a standard of care, we should now be moving toward SPECT/CT as our standard of care. The presentations at this year's SNMMI meeting reinforce this belief. At the same time, we need more outcomes and effectiveness data before SPECT/CT will be properly reimbursed so it can achieve more widespread routine clinical use.

Alan H. Maurer, MD
Temple University School of Medicine, Philadelphia, PA